Residual Stress Interference by Two Micro-Vickers Indentations

Ouk Sub Lee*

(*Received July 24, 1996*)

An electron beam moiré method is employed to measure the residual strain produced by a Vickers indenter in a WC-4.7wt.% Co specimen. Line gratings 57μm wide by 45μm high, with a pitch of 87nm, are written by electron beam lithography. Two interior regions of the grating are loaded by the micro-Vickers indenter with 9.8N for 30s. The residual stress interference phenomena caused by two impressions of the Vickers indenter are estimated by using the displacement fringes recorded with the aid of an electron beam moiré (EBM) technique. The measured residual stresses are fitted to the theoretical values estimated by two available models such as Yoffe model and CME (Chiang-Marshall-Evans) model.

Key Words: Chiang-Marshall-Evans (CME), Electron Beam Moiré Method (EBM), Gratings, Micro-Vickers Impression, Lithography, Micro-Vickers Indentation, Nanoscale Displacement, Residual Stress, Scanning Electron Microscope (SEM), Yoffe Model

1. Introduction

Because of its simplicity, the micro-Vickers indentation technique has been used for many years to characterize fracture and deformation processes in hard materials such as carbides and glasses (Marshall & Lawn 1979). Furthermore, it has been claimed that fracture toughness can be successfully estimated from the micro-Vickers indentation results even when there exists pronounced experimental data scatter. No one has experimentally explained this matter until the present time, since the measurements are carried out on a micrometer scale.

More recently, the residual stresses in soda-lime glasses were measured using the deflection method and X-ray diffraction, and both were found to agree with those obtained by the pointed-indentation technique (Chandrasekar & Chaudhri 1993) in which the theoretical background was adopted from two models (Yoffe 1982, Chiang, Marshall & Evans (CME) 1982). The stress fields derived from the two models were developed basically for the round indenter. However, CME provided a relationship which could be useful for pyramidal indentations while considering a hemispherical plastic zone around a Vickers pyramidal indentation. In this context, we attempt to adopt the Yoffe model as a candidate for describing the stress field around a Vickers indentation.

However, it is interesting to note that the two models predict different stress distributions, i. e., compressive (Yoffe) and tensile (CME) tangential surface stresses at the vicinity of the indent under identical loading. However, the tangential surface residual stresses (TSRS) under full unloading are predicted as being tensile in nature by the two models. The Yoffe model does not include the plastic zone at the surface of specimen around the impression, while the CME model allows large plastic zones below the indentation as well as the specimen surface around the indent. Furthermore, controversy on the detailed deformation mechanism in the region around various indenter impressions persists.

The main purpose of this paper is to measure nanoscale residual deformation around two micro-Vickers impression in a hard material specimen.

* Mechanical Engineering Department Inha University Inchon, 402-751 Korea

The electron beam moiré (EBM) technique (in which the pitches of specimen line and reference gratings were 87 and 76nm, respectively) is used to measure residual stress interference by two micro-Vickers indentations after full unloading of the two micro-Vickers indenters. The measured residual strains at the vicinity of an apex of micro-Vickers impressions are compared to those estimated using the Yoffe and the CME models. The strain field interfered by residual stresses produced by two micro-Vickers impressions are also measured using the EBM method and compared to those predicted by the Yoffe model. The technical information obtained in this paper will provide useful insight into understanding the scatter of fracture toughness determined experimentally with the aid of the micro-Vickers indentation technique and by using linear elastic fracture mechanics(LEFM). LEFM estimation in this case does not include the effect of residual stress distribution around the indentation on fracture toughness. Detailed information about the residual stress distribution will help determine more accurate fracture toughness values to reduce the scatter of experimental data.

2. Theoretical Background

The pertinent equations for TSRS within the elastic region around a Vickers impression are derived based on the residual stress fields given by the Yoffe and CME models, respectively, as follows:

$$TSRS_{Yoffe}=\frac{B(1+7\nu)}{Er^3} \tag{1}$$

$$TSRS_{CME}=\frac{H(1-\nu)(1-2\nu)}{E(1-m)\Omega^2}\times\left[\frac{1}{1+3\ln\beta}\left(3\beta\ln\beta-\frac{1}{2}\beta+\frac{3}{2}-\frac{\beta^3}{4\Omega^2}\right)-(\beta-1)-(1-m_r)\left(\frac{1}{\Omega^2}-1\right)\right] \tag{2}$$

where B=a constant representing the strength of the field (this will be estimated later in the next section); r=radial distance from the center of ball indentation; E=elastic modulus; ν= Poisson's ratio; H=hardness; m=free surface correction factor for peak load; m_r=free surface correction factor for residual stress; Ω=normalized radial distance from the center of ball indentation (= r/a); β=normalized plastic zone size(=b/a); and b=plastic zone size (this will be measured later in the next section) around indenting impression.

The relation between $\bar{a}$ and as follows:

$$a=\text{radius of ball indentation}=\bar{a}\times(\cot(\psi)/4.44)^{1/3} \tag{3}$$

where

$\bar{a}$=half diagonal of the Vickers impression; and ψ =half included angle between opposite faces of the indenter pyramid (=68°).

3. Experimental

3.1. Specimen material and EBM grating

The material used in this study is tungsten carbide with 4.7 wt.% cobalt as a binder (WC4.7Co). The modulus of elasticity and Poisson's ratio are 620 GPa and 0.22, respectively. The nominal size of the tungsten carbide skeleton is 1-5μm. A typical microstructure taken by using scanning electron microscope (SEM) is shown in Fig. 1.

To free the specimen surface from residual stresses, a 0.1mm layer (including 0.02mm deep skin in which residual stresses by EDM procedure

Fig. 1 A typical micrograph of WC4.7Co taken by SEM.

Fig. 2 A typical image of gratings in a 2000× pattern at a magnification of 60000× on SEM.

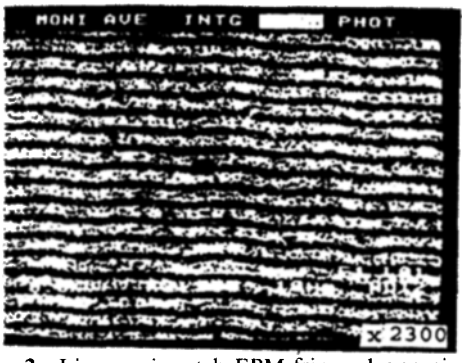

Fig. 3 Linear mismatch EBM fringes by specimem line gratings (pitch=87nm) and scanning lines of EB (pitch=76nm) (grating area=57μm wide by 45μm high).

may exist) is carefully polished away with 0.25μm diamond particles.

The second step is the application of a 100nm thin polymethylmethacrylate (PMMA) coating on the mirror surface specimen. This is achieved by spinning 2% volume PMMA (molecular weight of 950000 in chlorobenzene) at a speed of 2250 rpm for 30sec. The PMMA coating serves as an electron beam (EB) resist. The specimen is then baked on a hot plate for 90 minutes at 171℃. Some critical information on the writing of line gratings are as follows: time gap between baking and writing=3 hours; writing duration=220 s; probe current=4 pA, vacuum of SEM=4.8×10^{-6} torr; accelerating voltage of SEM=20KeV; and filament current of SEM=255μA. The general procedure for producing the line gratings is described in (Lee & Read 1995). A typical image of line gratings in a 2000× pattern recorded on an SEM at a magnification of 60000× is shown in Fig. 2. The wandering in line gratings appearing in Fig. 2 is due to a wavy motion of the incident EB and the random nature of electron backscattering in the SEM.

3.2. EBM fringe patterns

In the EBM method, the scan pattern of the SEM acts as a reference grating to produce EBM fringes associated with specimen line gratings written on the thin PMMA resist. The reference pitch can be varied by adjusting either the magnification of the SEM or the number of scan lines in the image. Figure 3 shows a small grating area 57μm wide by 46μm high covered with EBM fringe pattern in the WC4.7Co specimen. The EBM fringes shown in Fig. 3 are generated by the mismatch in pitches between specimen line gratings Ps=87nm and scanning lines of EB P_r=76nm.

4. Results and Discussion

The surface residual deformations produced by Vickers indentation were recorded using the EBM method. In the EBM method, we can modulate the measurement sensitivity by adjusting the pitch of specimen line gratings and/or reference gratings. Very fine specimen line gratings as shown in Fig. 2 were needed since the actual surface residual deformation produced by the Vickers indentation was very small.

Figure 4 (a), (b), (c) show three EBM fringe patterns (at a magnification of 2000× and 1100×

Fig. 4(a) EBM fringe patterns by linear mismatch and residual deformation at 2000× on SEM.

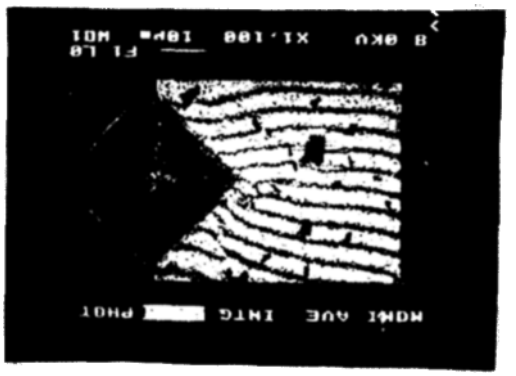

Fig. 4(b) EBM fringe patterns by linear mismatch and residual deformation at 1100× on SEM.

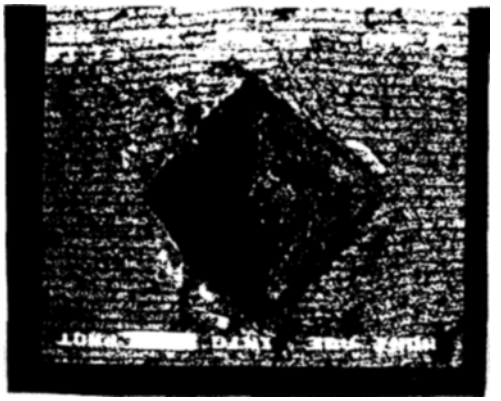

Fig. 4(c) EBM fringe patterns by linear mismatch and residual deformation at 2000× on SEM.

on SEM) appearing around the Vickers indenting impression after removing the indenter. The indenting load and time were 9.8 N and 30 sec, respectively. The changes in the EBM fringe pattern (comparing to the EBM linear mismatch fringes) near the vicinity of the micro-Vickers impression is clearly visible in Fig. 4. The non-symmetric fringe patterns around the apex of the indenter shown in Fig. 4(a) may be caused by the heterogeneous microstructure of the tungsten carbide specimen. It is interesting to note that the 1100× fringe patterns shown in Fig. 4(b) show more pronounced changes than those appearing in the 2000× fringe patterns shown in Fig. 4(a). Generating clear fringe patterns by modulating the magnification of the SEM is found to be very important in reducing experimental error. The difference in the shape of fringe patterns according to various magnifications of the SEM is due to the modulations caused by the electron beam intensity. Figure 4(c) shows the changes in fringe patterns at the four corners of a micro-Vickers indentation located in the center of the grating.

The half diagonal of the Vickers impression ā and the radius of the ball indentation a were 15 and 6.75μm, respectively. Strain measurements were carried out at 6 positions along a radial line (x-axis) passing the center and the apex of the micro-Vickers impression as shown in Fig. 5.

The displacement ($N\times p$ where N=fringe order number by residual displacement and linear mismatch EBM fringes, and p=pitch of reference gratings) along each of the vertical lines were fitted to polynomials of six degrees. The residual strains along vertical lines, ε_{yyres}, were estimated from the displacement values as

$$\varepsilon_{yyres}=p\frac{dN}{dy}-constant \tag{4}$$

where constant=$p\times dN'/dy$; and N'=fringe order number of linear mismatch EBM fringe patterns.

A constant B and the plastic zone size appearing in Eqs. (1) and (2), were respectively estimated as 1.57×10^{-6} and 2μm. We took the B value as an average of six values evaluated at six different positions along the x-axis. 2μm were

Fig. 5 A coordinate system set at apex for locating various positions where strain measurements are carried out.

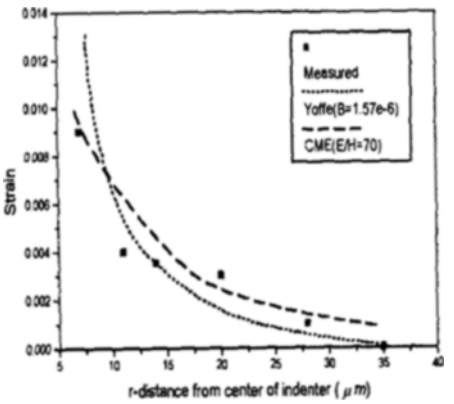

Fig. 6 Tangential surface residual strain determined by the EBM method and two models.

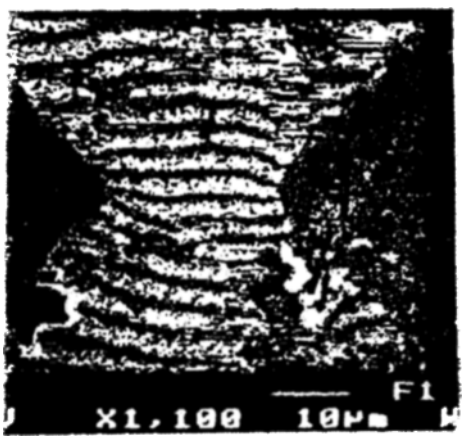

Fig. 7 EBM fringe patterns by linear mismatch and residual deformation at 1100× on SEM.

Fig. 8 An example of location of two-Micro Vickers impressions

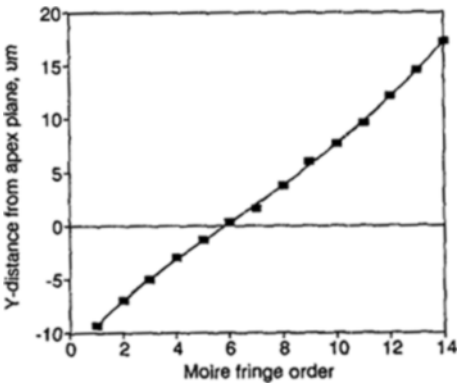

Fig. 9 EBM fringe displacement along y-line at $x=0.61\,\mu$m from apex of left-side impression.

identified as the permanently deformed region in PMMA coating at the vicinity of the apex of the micro-Vickers impression.

Figure 6 shows the TSRS estimated with the aid of the EBM technique and the two theoretical models (such as the Yoffe and CME models).

Figure 7 shows EBM fringe patterns at a magnification of 1100× on SEM appearing around two Vickers indenting impressions after removing the indenter. The indenting load and time were 9.8 N and 30 sec, respectively. The change in EBM fringe pattern (comparing to the EBM linear mismatch fringes and fringe patterns by a single micro-Vickers impression) near the vicinity of the micro-Vickers impression is clearly visible in Fig. 7.

The TSRS field produced by two micro-Vick-

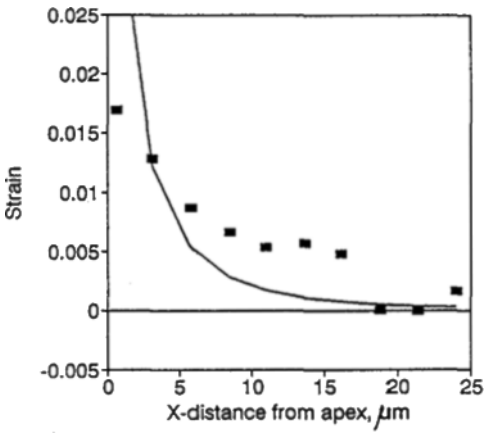

Fig. 10 Comprarison of experimental strain (along $x=0$ line) to those obtained by Yoffe model.

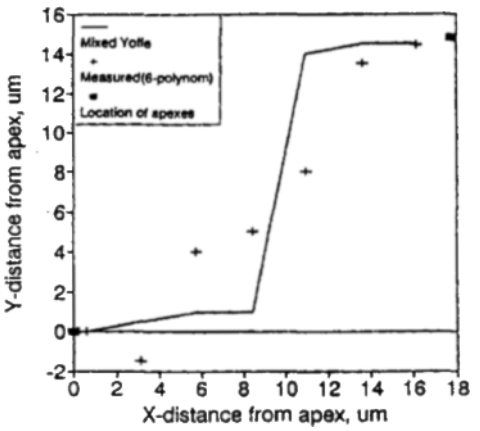

Fig. 11 Location of maximum ε_{yy} between two indenters in a WC4.7Co specimen.

ers indentations at varying locations in the grating areas were derived using Eq. (1) with a proper coordinate transformation. The two-indentations were located at a distance of 18μm along the x and 15μm along the y directions, respectively, as shown in Fig. 8. Figure 9 shows the EBM fringe displacements measured along the y-axis at $x=0.609\mu$m from the apex of the left-side impression. A curve fitted by using the 6-degree polynomial is shown in Fig. 9. Equation (4) was employed to estimate the strain appearing in Fig. 10. A comparison of experimental strain fields along the $x=0$ line to those of the Yoffe model is also shown in Fig. 10. Both the superposed Yoffe model and a single Yoffe model are found to agree well with the experimental measurements. The 15μm distance of the indenter in the y direction may be far enough to neglect the interference between two indentations. The CME model could not be utilised here due to the difficulties of accurate estimation of correction factors in the model. Figure 11 shows the location of maximum residual strains which were caused by the two micro-Vickers indentations in a WC4.7Co specimen. The predictions by the model were found to be in good agreement with the experimental results.

5. Conclusion

An EBM method has been successfully applied to measure very small residual deformation on the order of a few nm in a WC4.7Co specimen. It was found that the Yoffe and CME models successfully predicted the TSRS field around a micro-Vickers impression. It was also found that the Yoffe model can reasonably predict the TSRS field interfered by two Vickers indentations after full unloading.

Acknowledgment

This work is supported by the Korea Ministry of Education through Mechanical Engineering Research Fund (ME 94-C-10)

References

Chandrasekar, S. and Chaudhri, M. M., 1993, "Indentation Cracking in Soda-Lime Glass and Ni-Zn Ferrite Under Knoop and Conical Indenters and Residual Stress Measurements," *Philosophical Magazine A* 67, pp. 1187~1218.

Chiang, S. S., Marshall, D. B. and Evans, A. G., 1982, "The Response of Solids to Elastic/Plastic Indentation, 1. Stresses and Residual Stresses," *J. Appl. Phys.* 53, pp. 298~311.

Lee, O. S. and Read. D. T., 1995, "Micro-Strain Distribution Around a Crack Tip by Electron Beam Moiré Methods," *KSME Journal*. Vol. 9, No. 3. pp. 298~311.

Marshall, D. B. and Lawn, B. R., 1979, "Resid-

ual Stress Effects in Sharp Contact Cracking," *Journal of Materials Science* 14, pp. 2001~2012.

Yoffe, E. H., 1882, "Elastic Stress Fields Caused by Indenting Brittle Materials: Philosophica Magazine A 46," pp. 617~628.